J. Fluid Mech. (1980), *vol.* 99, *part* 2, *pp.* 365–382
Printed in Great Britain

A finite-rate theory of resonance in a closed tube: discontinuous solutions of a functional equation

By BRIAN R. SEYMOUR

Department of Mathematics and Institute of Applied Mathematics and Statistics, University of British Columbia, Vancouver, Canada

AND MICHAEL P. MORTELL

Registrar's Office, University College, Cork, Ireland

(Received 21 June 1979 and in revised form 28 November 1979)

The only solutions to date which describe nonlinear resonant acoustic oscillations are those for which the distortion of the travelling waves is negligible. Many experiments do not comply with this small-rate restriction. A finite-rate theory of resonance for an inviscid gas, in which the intrinsic nonlinearity of the waves is taken into account, necessitates the construction of periodic solutions of a nonlinear functional equation. This is achieved by introducing the notion of a critical point of the functional equation, which corresponds physically to a resonating wavelet. In a finite-rate theory a wave may break in a single cycle in the tube, and thus there may be more than one shock present even at fundamental resonance. Discontinuous solutions of the functional equation are constructed which satisfy the weak shock conditions.

1. Introduction

This paper discusses small-amplitude resonant, and near-resonant, oscillations of an inviscid gas in a closed tube when the propagating waves are intrinsically nonlinear. Then there is distortion of the wave as it moves along the tube. We refer to such oscillations, which can be produced by increasing either the driver frequency or the amplitude, as finite-rate oscillations. All extant theories of resonance in a closed tube, with the exceptions of Mortell (1971) and Seymour & Mortell (1973), have made a small-rate assumption. A consequence of this is that all wave distortion is assumed negligible. Seymour & Mortell (1973) showed that, in the finite-rate limit, the problem of calculating the propagating signal is reduced to finding periodic solutions of a functional equation. Continuous periodic solutions were found in Mortell & Seymour (1979). Here a new technique for constructing discontinuous solutions of the functional equation is introduced. Because of the evolutionary nature of the functional equation, these discontinuities satisfy the weak shock conditions.

The acceleration rate in any experiment is characterized (see Mortell & Seymour 1979) by the similarity parameter $A = 2\pi(\gamma+1)\epsilon\omega^2$, where ϵ is the ratio of piston amplitude to tube length, ω is the (dimensionless) piston frequency and γ is the gas constant (1·4 for air). We conclude here that when $A < 0{\cdot}08$ an experiment is in the small-rate range, while $A > 0{\cdot}08$ defines the finite-rate range. Seymour & Mortell (1973) explicitly pointed out the occurrence of the small-rate assumption in the derivation of theories up to that time, and the consequent restrictions on the experimental

0022-1120/80/4490-1540 $02.00

parameters. Recently, Chester has criticized the comparison of experiments in which intrinsic nonlinearity is present with a theory which is *not* intrinsically nonlinear, see Brocher (1977).

Most experiments reported to date have been in the small rate range. The earliest significant experiments, those of Lettau (1939), had an amplitude $\epsilon = 0{\cdot}0028$, and were in both the small- and finite-rate ranges as frequencies up to the fourth mode were used with $0{\cdot}01 < A < 0{\cdot}17$. The experiment reported by Saenger & Hudson (1960) was at the fundamental resonance with $\epsilon = 0{\cdot}0019$. Their conclusion that, to first order, the periodic shock waves have constant strength within the tube and travel uniformly in either direction is consistent with their small rate value of $A = 0{\cdot}0075$. Gulyayev & Kusnetsov (1963) note that in their experiment the instantaneous pressure rise within the shock changes along the duct – a finite rate effect. They have $\epsilon = 0{\cdot}011$ which gives $A = 0{\cdot}04$ at fundamental resonance. The experiment of Galiev, Ilgamov & Sadykov (1970), for which $\epsilon = 0{\cdot}0163$ and $A = 0{\cdot}081$ near the fundamental frequency, were just in the finite-rate range, as were those of Sturtevant (1974) with $\epsilon = 0{\cdot}0147$. In neither case can we say if shock strengths vary along the tube, since measurements are reported from a single location. Sturtevant (private communication) has also conducted experiments with CO_2 for which $\epsilon = 0{\cdot}0268$ ($A = 0{\cdot}096$) and with Freon 11 for which $\epsilon = 0{\cdot}0457$ ($A = 0{\cdot}160$), both in the finite-rate range. In the latter case our theory predicts that the response curve does not close on the right (see figure 1 here and Mortell & Seymour 1979). This was not tested in the experiments. Finally, the experiments of Zaripov & Ilgamov (1976) covered the whole finite-rate range with frequencies up to the third mode for $\epsilon = 0{\cdot}023$ and $0{\cdot}04 < A < 0{\cdot}93$. Their figure 4 would seem to indicate a difference in shock strength at different locations in the tube. They also note that, for amplitudes of 0·4 bar and higher, changes of waveform take place. However, their results should be interpreted with some care, since the amplitude $\epsilon = 0{\cdot}023$ was achieved with a cone reducer and is only an effective amplitude.

On the theoretical side, Betchov (1958), noting Lettau's (1939) small rate experiments, postulated the form of the solution and showed that, for an inviscid gas, the amplitude at resonance is finite and determined by nonlinear effects. In a little-quoted paper, Gorkov (1963) gives a method of solution (not unlike that of Chester 1964) in which shocks arise naturally in a frequency band about resonance. Interestingly, he avoided quantitative comparison of his theoretical results with the experiments of Gulyayev & Kusnetsov (1963) on the grounds that their amplitudes are large enough to warrant higher approximations in his theory!

One of the most influential papers on the subject of resonant acoustic oscillations is that of Chester (1964). He gives a deductive argument in which the transition from a continuous acoustic oscillation to one involving shock waves arises naturally. The basis of Chester's theory is that the disturbance in the body of the gas is an acoustic oscillation, so that the particle velocity $\bar{u}(x,t)$ has the representation

$$\bar{u}(x,t) = a_0 f(t - x/a_0) - a_0 f(t + x/a_0), \tag{1.1}$$

where a_0 is the sound speed in a suitable reference state. The implication of (1.1) is that waves in the tube propagate without distortion. Then the refinement of acoustic theory given by Chester is simply to ensure that the boundary condition at the piston is properly satisfied in order to determine the propagating signal f in (1.1).

The finite-rate theory, which here is used to analyse discontinuous oscillations in the linear resonance region, has previously been used to construct continuous, nonlinear, periodic oscillations (Mortell & Seymour 1979). This theory, which includes the effects of nonlinear distortion, is additionally valid at *any* frequency, and hence gives a certain unity which previously had been lacking.

2. Formulation

A pipe, one end of which is closed while at the other there is an oscillating piston, contains a column of gas of length L in some reference state. The pressure and density are measured from (and non-dimensionalized with respect to) the reference state (p_0, ρ_0) with the associated sound speed a_0. Then, in terms of the variables $a_0 u$, $\rho_0 a_0^2 p$, $\rho_0 \rho$, Lx and $La_0^{-1} t$, the governing equations in Lagrangian form are

$$\frac{\partial u}{\partial t} + \frac{\partial p}{\partial x} = \frac{\partial}{\partial t}[(1+e)^{-1}] - \frac{\partial u}{\partial x} = 0, \tag{2.1}$$

where $e(=\rho-1)$ is the condensation, γp the excess pressure ratio and u the particle velocity. In terms of these variables, the equation of state for the isentropic flow of an ideal gas is

$$p = \gamma^{-1}[(1+e)^{\gamma} - 1] = e + (M-1)\, e^2 + O(e^3), \tag{2.2}$$

where $M = \frac{1}{2}(\gamma+1)$ and γ is the ratio of specific heats.

The end $x = 0$ is closed, so that $u(0,t) = 0$, while at $x = 1$ there is a periodic piston displacement of the form $\epsilon \bar{h}(\omega t)$. Here $\epsilon(\ll 1)$ is the ratio of the maximum piston displacement to the column length, L, and $\bar{h}$ has unit period in ωt, so that

$$\bar{h}(y+1) = \bar{h}(y).$$

Thus ω^{-1} is the non-dimensional period of the piston. In terms of the particle velocity, the boundary condition at the piston is

$$u(1,t) = h(\omega t), \tag{2.3}$$

where $h(\omega t) = \epsilon\omega \bar{h}'(\omega t)$, and hence h has zero mean over a period. For periodic gas motions, the means of u and p are also zero.

Seymour & Mortell (1973) and Mortell & Seymour (1979) have shown that, for small piston speeds $\epsilon\omega$ but for any frequency ω, the motion of the gas can be described in terms of solutions of the functional equation

$$\left.\begin{aligned} f(\eta) &= f(s) + h(\eta), \\ \eta &= s + 2\omega + 2\omega M f(s), \end{aligned}\right\} \tag{2.4}$$

where f has unit period and zero mean value. The pressure and particle velocity are given at any position in the tube, in terms of f, to first order, by

$$p = -f(\beta) - g(\alpha), \quad u = f(\beta) - g(\alpha), \tag{2.5}$$

and

$$\alpha = \omega(t-x) - \omega M x g(\alpha), \quad \beta = \omega(t+x-1) + \omega M(x-1) f(\beta), \tag{2.6}$$

where g is related to f by

$$g(\phi + \omega + \omega M f(\phi)) = f(\phi). \tag{2.7}$$

When equation (2.4) is linearized, by setting $M = 0$, it has no bounded periodic solution for $\omega = \omega_n = \frac{1}{2}n$, $n = 1, 2, 3, \ldots$, the linear resonant frequencies. Defining, for any n,

$$F = 2\omega Mf + \Delta, \quad H = 2\omega Mh \quad \text{and} \quad \Delta = 2(\omega - \omega_n), \tag{2.8}$$

equations (2.4) become

$$F(\eta) = F(s) + H(\eta), \quad \eta = s + F(s), \tag{2.9}$$

where F has unit period and must satisfy the mean condition

$$\int_0^1 F(\eta)\, d\eta = \Delta. \tag{2.10}$$

The basic functional equation (2.9) can be regarded as the product of two mappings:

$$T1: (s, F(s)) \to (\eta, \hat{F}(\eta)), \tag{2.11}$$

where $$\hat{F}(\eta) = F(s(\eta)), \quad \eta = s + F(s);$$

and

$$T2: (\eta, \hat{F}(\eta)) \to (\eta, F(\eta)), \tag{2.12}$$

where $$F(\eta) = \hat{F}(\eta) + H(\eta).$$

$T1$ can be regarded as a 'simple-wave mapping'. The function $\hat{F}(\eta)$ represents the distorted signal returning to the piston after reflexion from $x = 0$, but before it has been reinforced by the piston motion. $T2$ then represents the action of the piston on $\hat{F}(\eta)$. A given function, defined over a unit interval, is a solution of equations (2.9) if it maps onto itself under the product $T2T1$. To be an acceptable physical solution it must also satisfy the periodicity condition and the mean condition (2.10), in which Δ is a measure of the detuning from a linear resonant frequency.

Before attempting to construct solutions of equations (2.9), it is instructive to consider the small-rate limit, defined by

$$|H| = 2M\epsilon\omega^2 |\bar{h}'| \ll 1, \tag{2.13}$$

when the functional equation (2.9) can be approximated by the ordinary differential equation

$$F_d(\eta)\, F_d'(\eta) = H(\eta). \tag{2.14}$$

The small-rate limit (2.13), in addition to limiting the modes for which equation (2.14) applies for a given amplitude ϵ, also limits the range of frequencies about each linear resonant frequency to $|\Delta| \ll 1$. These restrictions are noted explicitly by Seymour & Mortell (1973). All other theories of resonant oscillations have implicitly made the small rate assumption.

For the sinusoidal piston motion usually used in experiments

$$H(\eta) = A \sin(2\pi\eta), \tag{2.15}$$

where the similarity parameter $A = 4\pi M\epsilon\omega^2$. The integral curves of equations (2.14) and (2.15) in the (η, F) plane have the well-known form of the nonlinear pendulum:

$$F_d(\eta) = \pm [F_d^2(0) + 2A\pi^{-1} \sin^2(\pi\eta)]^{\frac{1}{2}}. \tag{2.16}$$

All solutions are even about $\eta = \frac{1}{2}$ with $F_d'(\frac{1}{2}) = 0$. The saddle points at $(0, 0)$ and $(1, 0)$ are connected by the separatrices

$$z^{\pm}(\eta) = \pm (2A/\pi)^{\frac{1}{2}} \sin(\pi\eta), \tag{2.17}$$

which enclose the centre at $(\frac{1}{2}, 0)$. For

$$|\Delta| \geqslant \int_0^1 z^+(\eta)\, d\eta = \left(\frac{8A}{\pi^3}\right)^{\frac{1}{2}} = \Delta_e(A), \tag{2.18}$$

the solution curves given by equation (2.16) are continuous and periodic, while for $|\Delta| < \Delta_e(A)$ there are no continuous periodic solutions. For frequencies such that $\Delta < \Delta_e(A)$ a discontinuous periodic solution is constructed using $z^{\pm}(\eta)$:

$$F_d(\eta) = \begin{cases} z^+(\eta), & 0 \leqslant \eta < \eta_s, \\ z^-(\eta), & \eta_s < \eta \leqslant 1. \end{cases} \tag{2.19}$$

The shock location at $\eta = \eta_s$ is determined by the mean condition (2.10) and yields

$$\cos(\pi\eta_s) = -\Delta/\Delta_e. \tag{2.20}$$

Thus $\eta_s \to 1$ (0) as $\Delta \to \Delta_e$ $(-\Delta_e)$. The small-rate solution (2.16) usually referred to as 'Chester's solution', was found independently by Gorkov (1963) and Chester (1964).

Continuous periodic solutions of the functional equation (2.9) are given in Mortell & Seymour (1979). There it is shown that the A–Δ plane is divided by a transition curve into regions where continuous periodic solutions exist and where they do not, the results being reproduced here in figure 1. It should be noted that for H given by equation (2.15) the transition curve is an even function of Δ about $\Delta = 0$ and $\Delta = \frac{1}{2}$. Hence all solutions can be represented in the strip $0 \leqslant \Delta \leqslant \frac{1}{2}$, $A \geqslant 0$. The first branch of the transition curve $\Delta = \Delta_t(A)$, $0 \leqslant A \leqslant 0{\cdot}12$, passing through $A = \Delta = 0$, defines the boundary of the linear resonant band, containing each linear resonant frequency ω_n. The parabolic nature of $\Delta_t(A)$ in the small-rate limit, $A \ll 1$, is confirmed by the formula (2.18) for $\Delta_e(A)$. The region $0 \leqslant \Delta \leqslant \Delta_l(A)$ of figure 1 is the linear resonance region, and coincides with $\Delta = \Delta_t(A)$ for $0 \leqslant A \leqslant 0{\cdot}08$. For piston motions with A and Δ in the linear resonance region, the propagating signal leaving $x = 1$ always contains at least one wavelet carrying an amplitude which completes a cycle in the tube in an integer multiple of the period of H. This definition of the linear resonance region will be made more precise in §4. In this paper, we construct the periodic motions in the linear resonance region.

3. Construction of multivalued invariant curves

The algorithm given in Mortell & Seymour (1979) for constructing continuous periodic solutions of equations (2.9) fails to yield solutions in the linear resonance region and a new approach is needed. Functional equations of the form (2.9) have received scant attention in the literature. Kuczma (1968) refers to their solutions as invariant curves, and gives various local properties. Some insight into the global properties of their solutions was obtained by Mortell & Seymour (1976), where two classes of exact solutions for piecewise linear functions, $H(\eta)$, were found. The key to constructing these exact solutions, which is further exploited here, is in recognizing that the role of the fixed points of the invariant curves is analogous to that of the critical points of the corresponding small-rate differential equation (2.14). Thus the local structure of the invariant curves can be classified in the neighbourhood of the fixed points. Two invariant curves emanating from each saddle point are found for $0 \leqslant \eta \leqslant 1$. When $|H| \ll 1$ their structure is similar to the separatrices (2.17) of equation (2.14). However, as $|H|$ increases, the invariant curves become multivalued.

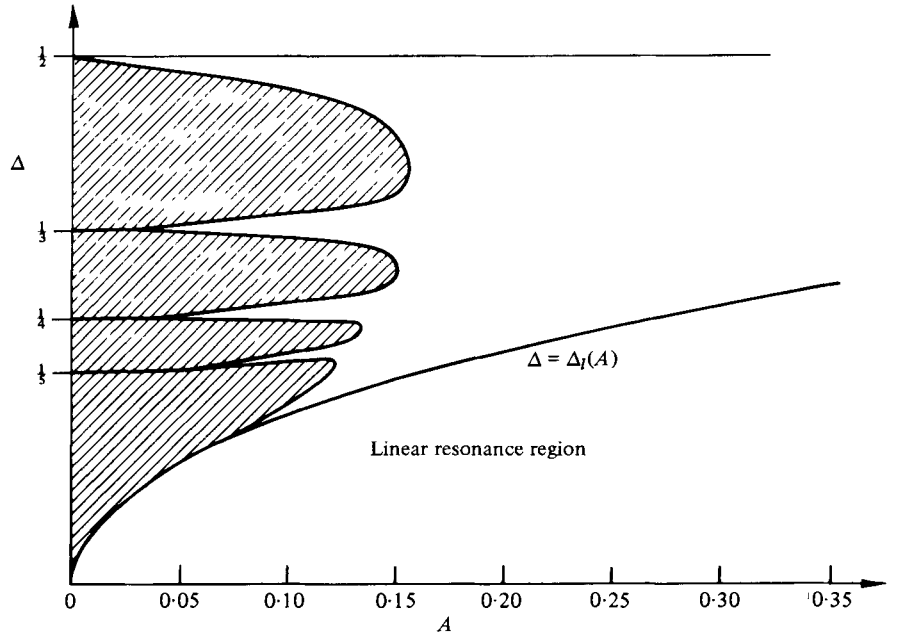

FIGURE 1. Transition curve in A–Δ plane bounding region of continuous periodic solutions (shaded), and the edge of the linear resonance region, $0 \leqslant \Delta \leqslant \Delta_l(A)$, considered in this paper.

It is convenient to distinguish between the invariant curves of equation (2.9), which we denote by $Z(\eta)$, and the physical solution, $F(\eta)$, which must be single-valued and also satisfy the mean condition (2.10). A fixed point (or critical point) of an equation of the form (2.9) is a point (η_c, Z_c) defined by

$$\eta = s = \eta_c \quad \text{when} \quad Z(\eta) = Z(s) = Z_c. \tag{3.1}$$

For equation (2.9) they are the points where

$$Z_c = H(\eta_c) = 0, \tag{3.2}$$

and are thus located at the zeros of the forcing function. Any physical solution containing a critical point must include a resonating wavelet in the propagating signal with the value $Z = 0$, corresponding, by definition (2.8), to

$$f = -\Delta/(2M\omega). \tag{3.3}$$

Then there is at least one point in the signal leaving $x = 1$ which completes one cycle in the tube in an integer multiple of the piston period. The frequency range about the linear resonant frequencies for which there is a resonating wavelet is the linear resonance region.

In order to classify the critical points and thereby study the local structure of solutions, we linearize the functional equation (2.9) about a critical point, for arbitrary $|H|$, to yield the autonomous differential equation

$$\frac{dZ}{dy} = \frac{\mu(Z+y)}{Z}, \tag{3.4}$$

where $y = \eta - \eta_c$ and $\mu = H'(\eta_c)$. Then, for $\mu > 0$ the critical point is a saddle point, and for $\mu < 0$ it is either a stable spiral or a node. The possible slopes of the invariant curves through a saddle point $(\eta_s, 0)$ are calculated by differentiating the functional equation (2.9) and setting $\eta = s = \eta_s$, yielding

$$\lambda^{\pm} = \tfrac{1}{2}[\mu \pm (\mu^2 + 4\mu)^{\frac{1}{2}}], \tag{3.5}$$

where $\lambda^{\pm} = Z'(\eta_s)$. Since $H(\eta_c) = 0$ and H has zero mean there is at least one saddle point in each period.

By taking the second derivative, with respect to s, of the first of equations (2.9) and eliminating $d\eta/ds$ we obtain

$$Z''(s) = [1 + Z'(s)]^3 [Z''(\eta) - H''(\eta)], \tag{3.6}$$

which yields, on setting $\eta = s = \eta_s$,

$$Z''(\eta_s) = \left[\frac{(1+\lambda^{\pm})^3}{(1+\lambda^{\pm})^3 - 1}\right] H''(\eta_s). \tag{3.7}$$

Similarly, as many derivatives of Z at a saddle point may be calculated as there are derivatives of H there. Hence the Taylor approximation to an invariant curve can be computed to any accuracy in the neighbourhood of a saddle point. This then overcomes the inherent difficulty of equations of the form (2.9), viz., that the solution must be known over a non-zero interval before it can be extended.

Two solutions emanate from any saddle point in the direction of increasing η, one with positive and one with negative slope. Without loss of generality we take $\eta_s = 0$. If $Z_0^+(s)$ is a known positive solution of equations (2.9) for $0 = \eta_s \leqslant s \leqslant s_1$, then equations (2.9) imply that $\eta > s$ and that $Z_0^+(\eta)$ is known for $0 \leqslant \eta \leqslant \eta_1$, where $\eta_1 = s_1 + Z_0^+(s_1) > s_1$. By repeating this procedure the solution can be further extended to the interval $0 \leqslant \eta \leqslant \eta_2$, where $\eta_2 = \eta_1 + Z_0^+(\eta_1) > \eta_1$. Hence, by repeated use of the mapping (2.9), any non-zero segment of solution curve containing the saddle point at $\eta = 0$ may be extended to the interval $0 \leqslant \eta \leqslant 1$. (This holds only if $Z_0^+(s) \geqslant 0$ for $0 \leqslant \eta = s + Z_0^+(s) \leqslant 1$, which can easily be verified.) The initial segment containing the saddle point is constructed by the Taylor series. We note that the subsequent mappings are exact. The only error introduced is in truncating the Taylor series.

The negative solution from $\eta_s = 0$, in the direction of increasing η, $Z_0^-(\eta)$, can be calculated either from a mapping scheme similar to that used to find $Z_0^+(\eta)$ (though now $0 \leqslant \eta \leqslant s$), or by noting that, through equations (2.9),

$$Z_0^-(\eta) = H(\eta) - Z_0^+(\eta). \tag{3.8}$$

Two further solutions, emanating from $\eta_s = 1$ in the direction of decreasing η, can similarly be constructed on $[0, 1]$ by extending the Taylor approximations to the two solutions near $\eta_s = 1$. We denote these by $Z_1^{\pm}(\eta)$, with $Z_1^+(\eta) > 0$ near $\eta = 1$. If the piston motion has the symmetry $H(\eta) = -H(1-\eta)$, it is easy to show that, when $Z(\eta)$ is a solution, $-Z(1-\eta)$ is also. Hence, using equation (3.8), $Z_1^{\pm}(\eta)$ can also be written in terms of $Z_0^+(\eta)$ as follows:

$$Z_1^+(\eta) = H(\eta) + Z_0^+(1-\eta) \tag{3.9}$$

and

$$Z_1^-(\eta) = -Z_0^+(1-\eta). \tag{3.10}$$

For definiteness we consider the piston motion given by equation (2.15). The structure of the four solution curves $Z_0^{\pm}$, $Z_1^{\pm}$ depends strongly on the magnitude of the similarity parameter A. In the small rate range, $0 < A < A_1$, the curves Z_0^+ and Z_1^+

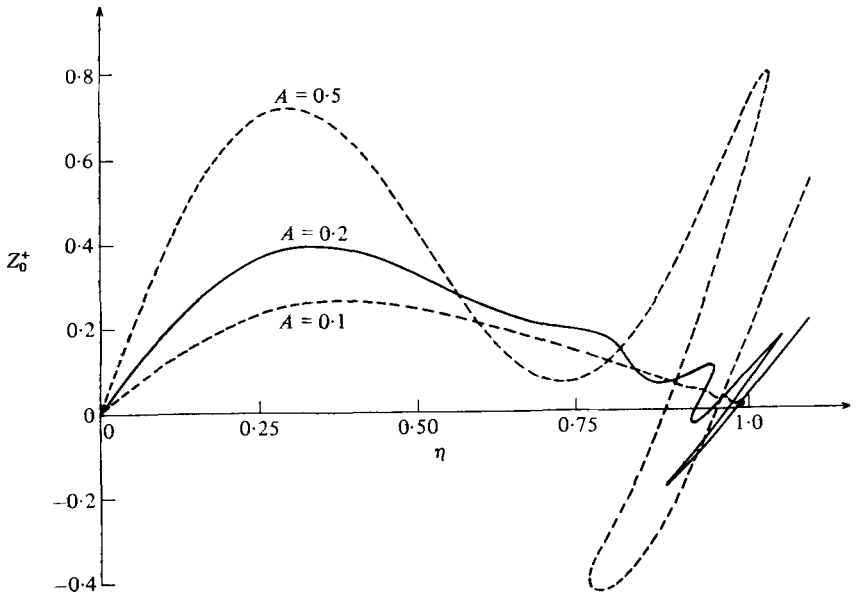

FIGURE 2. Finite-rate solution curves $Z_0^+(\eta)$ for $H(\eta) = A\sin(2\pi\eta)$ when $A = 0{\cdot}1$, $0{\cdot}2$ and $0{\cdot}5$.

(and also Z_0^- and Z_1^-) are indistinguishable, i.e. there are two invariant curves connecting the saddle points $\eta = 0, 1$. These are direct analogues of the separatrices $z^{\pm}(\eta)$ for the differential equation (2.14). From numerical investigations we find that A_1 is approximately $0{\cdot}01$, though we have no proof of the existence of $A_1 > 0$. However, it is not until $A > 0{\cdot}08$ that Z_0^+ and Z_1^+ are distinguishable on a scale of physical interest; hence we take $A_1 = 0{\cdot}08$, corresponding to $\epsilon = 0{\cdot}014$ for the first mode and $\epsilon = 0{\cdot}005$ for the second mode.

When $A_1 < A < A_2$, where A_2 is approximately $0{\cdot}8$, we say A is in the finite-rate range. In this range the curve $Z_0^+(\eta)$ (and hence by (3.9) and (3.10), $Z_1^{\pm}$ and Z_0^-) is *multivalued* on $[0, 1]$; $Z(\eta)$ becomes multivalued whenever $|Z'(\eta)| \to \infty$, which, by equations (2.9), occurs whenever $1 + Z'(s) \to 0$. Then the 'breaking time' of some part of the propagating signal is less than its travel time in the tube. The finite-rate theory is presented here to cope with this distortion, which is clearly outside the scope of any small-rate (differential equation) theory. Multivalued solutions $Z_0^+(\eta)$ are illustrated in figure 2 for $A = 0{\cdot}1$, $0{\cdot}2$ and $0{\cdot}5$. For $A = 0{\cdot}1$ the multivalued loops are quite small, but become larger as A increases.

In the finite range, $Z_0^+(\eta)$ and $Z_1^+(\eta)$ are *distinct* and intersect an infinite number of times on $[0, 1]$. This is illustrated in figure 3 for $A = 0{\cdot}3$, where the multivalued loops of $Z_0^+(\eta)$ on $[\frac{1}{2}, 1]$ are intersected by $Z_1^+(\eta)$. By equations (2.9) and (3.9), $Z_0^+(\eta)$ and $Z_1^+(\eta)$ intersect at $\eta = y_0$ and y_1 where

$$y_1 = \tfrac{1}{2} \quad \text{and} \quad y_0 = y_1 - Z_0^+(y_1),$$

since $Z_0^+(y_0) = Z_0^+(y_1)$. There is a further point of intersection at $\eta = r_0$, $y_0 < r_0 < y_1$. Then

$$Z_0^+(r_i) = Z_1^+(r_i), \quad r_{i+1} = r_i + Z_0^+(r_i)$$

and

$$Z_0^+(y_i) = Z_1^+(y_i), \quad y_{i+1} = y_i + Z_0^+(y_i), \quad -\infty < i < \infty,$$

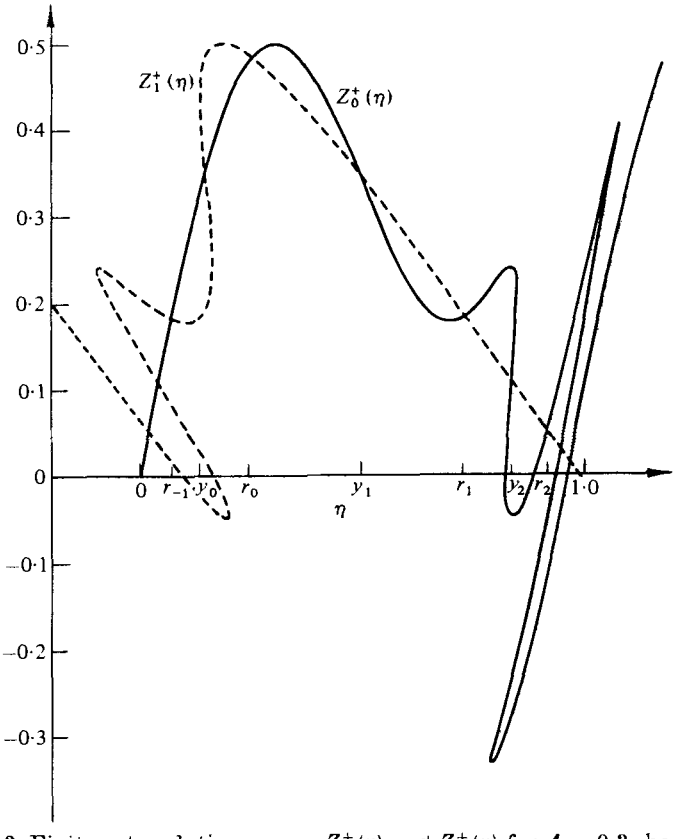

FIGURE 3. Finite-rate solution curves $Z_0^+(\eta)$ and $Z_0^+(\eta)$ for $A = 0{\cdot}3$ showing points of intersection given by equations (3.13) and (3.14).

define two sequences of points of intersection. These are the only points common to $Z_0^+(\eta)$ and $Z_1^+(\eta)$. The limit points of these points of intersection are the saddle points at $\eta = 0$ and $\eta = 1$. A class of exact solutions in which this property is explicitly demonstrated is given in Mortell & Seymour (1976). Note that the algorithm for generating solutions is not affected by the multivaluedness since it is a purely algebraic process, independent of $Z'(\eta)$, in the multivalued region.

4. Construction of periodic solutions

In the finite-rate range, the invariant curves must be made single-valued before constructing the periodic solution to (2.9) and (2.10). The observation that multivalued solutions correspond to breaking waves indicates that single-valued solutions should be obtained by inserting shocks using an equal-area rule. This choice of discontinuities is consistent with the mappings $T1$ and $T2$, which are both area preserving, and the weak shock conditions. A composite of the two discontinuous 'separatrices' on [0, 1] joined by a further shock is chosen to satisfy the mean condition (2.10). It is then demonstrated that, on using the equal-area rule, this final discontinuous function is a solution of the functional equation (2.9). The direction of the jumps is

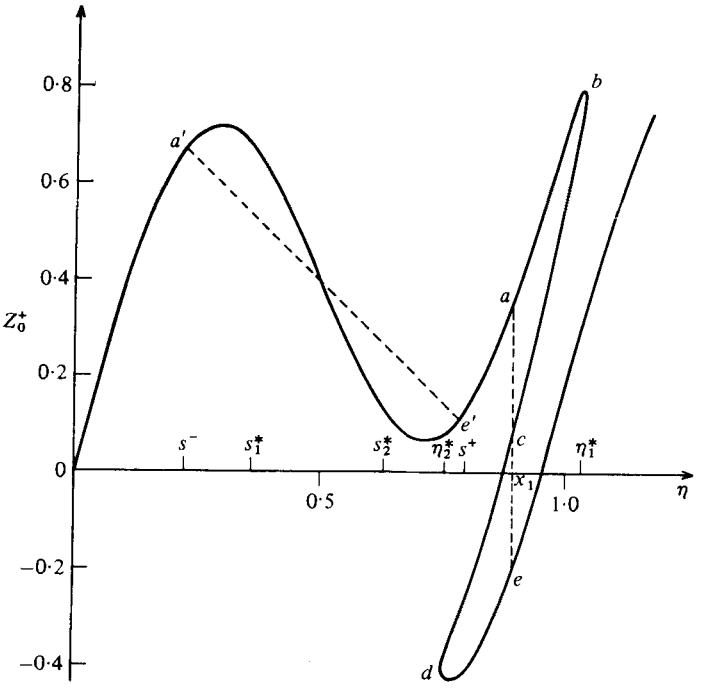

FIGURE 4. Discontinuities are inserted in multivalued loops to preserve area. The line $a'e'$ is mapped onto ae.

inherent in the functional equation, which includes the cumulative distortion over a cycle, and hence no appeal to an entropy condition is necessary.

4.1. *Discontinuous invariant curves*

In § 3 it was shown that, for $A > A_1$, the curve $Z_0^+(\eta)$ has an infinite number of multivalued loops on $[\frac{1}{2}, 1]$, each of which is intersected by the curve $Z_1^+(\eta)$. By equations (2.9), $|Z'(\eta)| \to \infty$ as $\eta \to \eta_1^*$ whenever $1 + Z'(s) \to 0$ as $s \to s_1^*$, where $\eta_1^* = s_1^* + Z(s_1^*)$. The multivalued loop on $[\eta_2^*, \eta_1^*]$ of $Z_0^+(\eta)$, illustrated in figure 4 for $A = 0{\cdot}5$, is the image of $Z_0^+(\eta)$ on $[s_1^*, s_2^*]$. A discontinuity is inserted at $\eta = x_1$, $\eta_2^* < x_1 < \eta_1^*$. The points marked a and e are the images of a' and e' at s^- and s^+ under the mapping (2.9). Thus, by equations (2.9),

$$x_1 = s^- + Z_0^+(s^-) = s^+ + Z_0^+(s^+), \tag{4.1}$$

equivalent to two of the weak shock conditions. The equal-area rule (see Whitham 1974) is the third shock condition and can be written in terms of Z as

$$\int_{s^-}^{s^+} Z(\eta)\, d\eta - \tfrac{1}{2}\{Z(s^+) + Z(s^-)\}(s^+ - s^-) = 0. \tag{4.2}$$

Equations (2.9) and (4.1) then imply that the area enclosed by the loop $abcde$ is

$$\int_{abcde} Z_0^+(\eta)\, d\eta = \int_{s^-}^{s^+} Z_0^+(s)\, ds + \tfrac{1}{2}\{Z_0^{+2}(s^+) - Z_0^{+2}(s^-)\} = 0, \tag{4.3}$$

by equations (4.1) and (4.2). Thus each multivalued loop in Z_0^+ is made single-valued by inserting a discontinuity which cuts off lobes of equal area. It can additionally

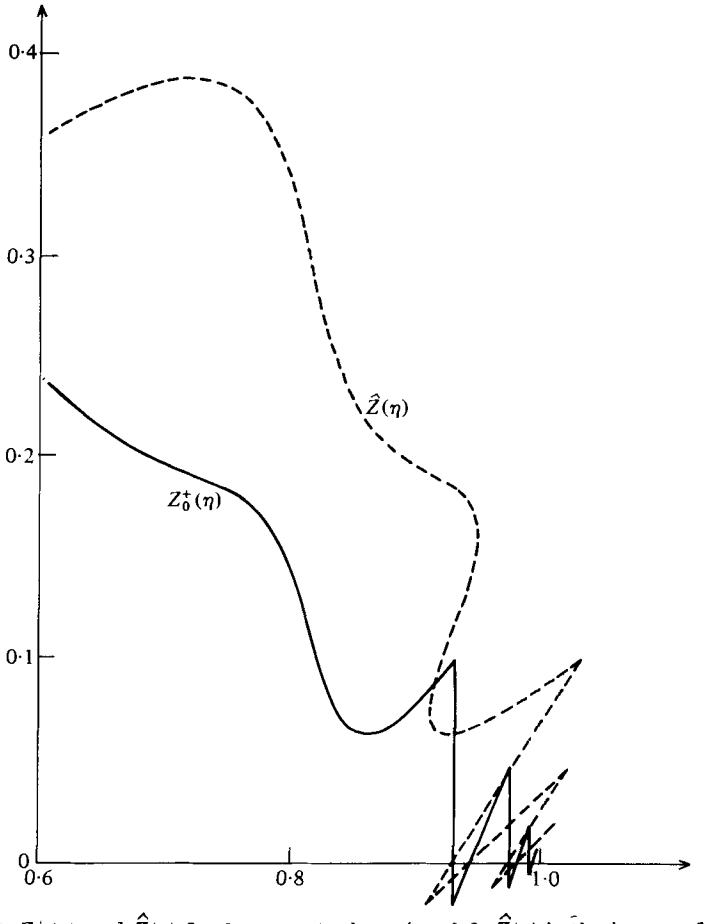

FIGURE 5. $Z_0^+(\eta)$ and $\hat{Z}(\eta)$ for $0 \leqslant \eta \leqslant 1$ when $A = 0{\cdot}2$. $\hat{Z}(\eta)$ is the image of $Z_0^+(\eta)$ under the simple wave mapping (4.5) which takes the ith shock onto the $(i+1)$st.

be shown that the areas bounded by Z_0^+ and Z_1^+ between successive points of intersection are all equal. Hence there is a discontinuity in Z_0^+ in each interval $[r_i, r_{i+1}]$, $i \geqslant j$, when Z_0^+ first becomes multivalued in the jth interval. This, in the finite-rate range, Z_0^+ contains an infinite number of shocks on $[\frac{1}{2}, 1]$ whose strengths tend monotonically to zero and their locations tend to $\eta = 1$ as $i \to \infty$. This is illustrated in figure 5 for $A = 0{\cdot}2$, which also exhibits the function $\hat{Z}(\eta) = Z_0^+(s(\eta))$. $\hat{Z}(\eta)$ is the distortion of $Z_0^+(\eta)$ under the simple wave mapping $T1$. Under this mapping the ith shock maps onto the $(i+1)$st shock, on using the equal-area rule. Thus $\hat{Z}(\eta)$ and $Z_0^+(\eta)$ have shocks of identical strengths at the same locations. Since, by $T2$,

$$\hat{Z}(\eta) = Z_0^+(\eta) - H(\eta),$$

the discontinuous function $Z_0^+(\eta)$ maps onto itself under equations (2.9) and the equal-area rule, and hence may be considered a discontinuous invariant curve.

In a similar manner, we construct discontinuous functions from the multivalued solutions Z_0^- and $Z_1^\pm$. However, it is easily seen that, of these three functions, only that derived from Z_1^- is a discontinuous solution of (2.9) and (4.2). Any discontinuity

introduced in Z_0^+ or Z_1^- is compressional and is maintained, while a discontinuity in Z_0^- or Z_1^+ produces a straight-line segment, corresponding to an expansion fan, under the mapping $T1$. The direction of the jumps in Z_0^+ and Z_1^- is consistent with that demanded by the entropy condition (Whitham 1974).

We have thus constructed two single-valued separatrices, Z_0^+ and Z_1^-, on [0, 1] in both the small- and finite-rate ranges. They are illustrated in figures 6 and 7 for $A = 0{\cdot}05$ and $A = 0{\cdot}3$. In the small-rate range the separatrices are the limiting curves of the continuous periodic curves, which do not contain fixed points of equations (2.9), that were constructed in Mortell & Seymour (1979). Several of these continuous curves are included in figure 6, which also includes the separatrices associated with the quadratic resonance at $\Delta = \frac{1}{2}$. The analysis for these latter curves is given in Mortell & Seymour (1980). Further analysis shows that there are also separatrices about $\Delta = \frac{1}{3}, \frac{1}{4}, \frac{1}{5}$. so that the continuous curves do not fill the whole region between the separatrices associated with $\Delta = 0$ and $\Delta = \frac{1}{2}$. In both the small- and finite-rate ranges, the separatrices Z_0^+ and Z_1^- correspond to the piston frequencies

$$\omega^{\pm} = \omega_n \pm \frac{1}{2}\int_0^1 Z_0^+(\eta)\,d\eta, \tag{4.4}$$

$$= \omega_n \pm \tfrac{1}{2}\Delta_l(A),$$

on using equations (2.8) and (2.10). If the applied frequency is such that

$$|\Delta| < \Delta_l(A) \tag{4.5}$$

there is no continuous solution of (2.9) which satisfies the mean condition (2.10). When $|\Delta| > \Delta_l(A)$ there is no longer an amplitude of the signal leaving $x = 1$ which completes a cycle in the tube in a multiple of the period of H. Hence $\Delta = \Delta_l(A)$ defines the edge of the linear resonance region and is equivalent to statement (3.3). It is illustrated in figure 1, which indicates that in the small-rate range

$$\Delta_l(A) \simeq \Delta_e(A) \simeq \Delta_t(A)$$

coinciding with the transition curve separating the regions in the A–Δ plane corresponding to continuous and discontinuous periodic solutions of equations (2.9) and (2.10). In the finite-rate range the edge of the linear resonance region does not correspond to the transition curve.

The area $\int_0^1 Z_0^+(\eta)\,d\eta$, defining the boundary of the linear resonance region, can be calculated, even in the finite-rate range, using only continuous portions of $Z_0^+(\eta)$. On noting equations (3.9), (4.3) and (4.4)

$$\Delta_l(A) = \int_0^1 Z_0^+(\eta)\,d\eta = \int_0^{r_1} Z_0^+(\eta)\,d\eta + \int_{r_1}^1 Z_1^+(\eta)\,d\eta$$

$$= \int_0^{r_1} Z_0^+(\eta)\,d\eta + \int_0^{1-r_1} [Z_0^+(\eta) - H(\eta)]\,d\eta.$$

The curve $\Delta = \Delta_l(A)$, calculated in this way, is plotted in figure 1.

4.2. *Solution in the linear resonance region*

In §§ 3 and 4.1 single-valued solution curves of equations (2.9) have been constructed which join the saddle points at $\eta = 0$ and $\eta = 1$. When the applied frequency, ω, is

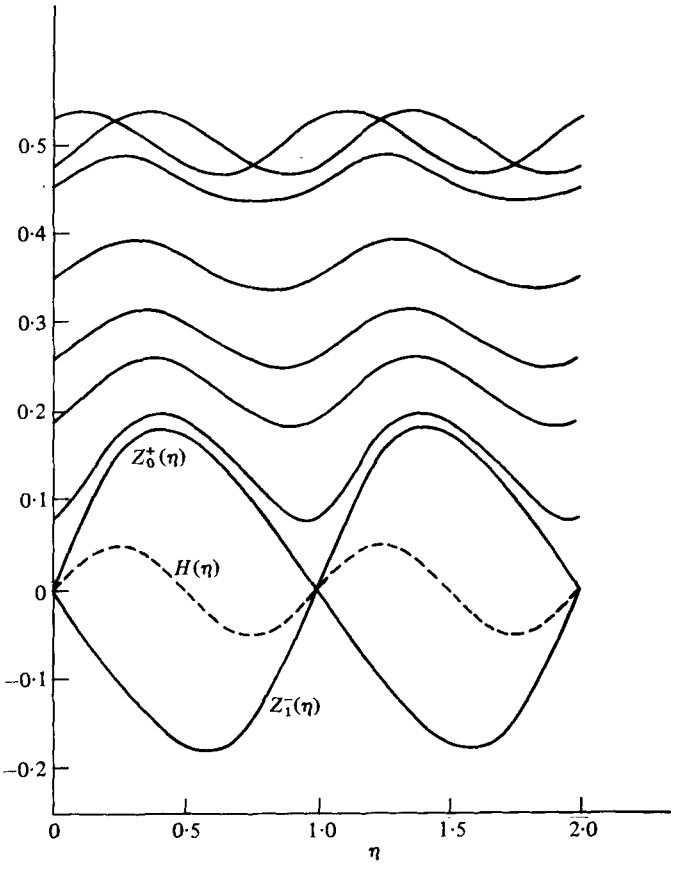

FIGURE 6. Small-rate Z–η plane for $A = 0{\cdot}05$. Solid curves are all solutions of equation (2.9) each corresponding to a different driving frequency.

in the range $|2(\omega-\omega_n)| = |\Delta| < \Delta_l(A)$ there is no single invariant curve, $Z(\eta)$, of equations (2.9) which satisfies the mean condition (2.10). Consequently, as in § 2 for the ordinary differential equation (2.12), we define the discontinuous function

$$F(\eta) = \begin{cases} Z_0^+(\eta), & 0 \leqslant \eta < x_s, \\ Z_0^-(\eta), & x_s \leqslant \eta < 1. \end{cases} \tag{4.6}$$

The location of the discontinuity, $x_s(\Delta)$, is chosen to satisfy the mean condition (2.10); for example,

$$x_s(0) = \tfrac{1}{2}, \quad x_s(\Delta_l) = 1 \quad \text{and} \quad x_s(-\Delta_l) = 0.$$

This additional discontinuity must also satisfy the weak shock conditions. By the construction of Z_0^+ and Z_1^-, equations (2.9) imply that for any $0 < x_s < 1$ there exist numbers s^- and s^+, where $0 < s^- < x_s < s^+ < 1$, such that

$$x_s = s^- + Z_0^+(s^-) = s^+ + Z_1^-(s^+). \tag{4.7}$$

Hence, since η varies continuously on $[0, 1]$, from equations (2.9)

$$F(x_s)^+ - F(x_s)^- = F(s^+) - F(s^-) = -(s^+ - s^-), \tag{4.8}$$

where $F(x_s)^+ = \lim_{\eta \downarrow x_s} F(\eta) = Z_1^-(x_s)$. Integrating the first of equations (2.9) with respect

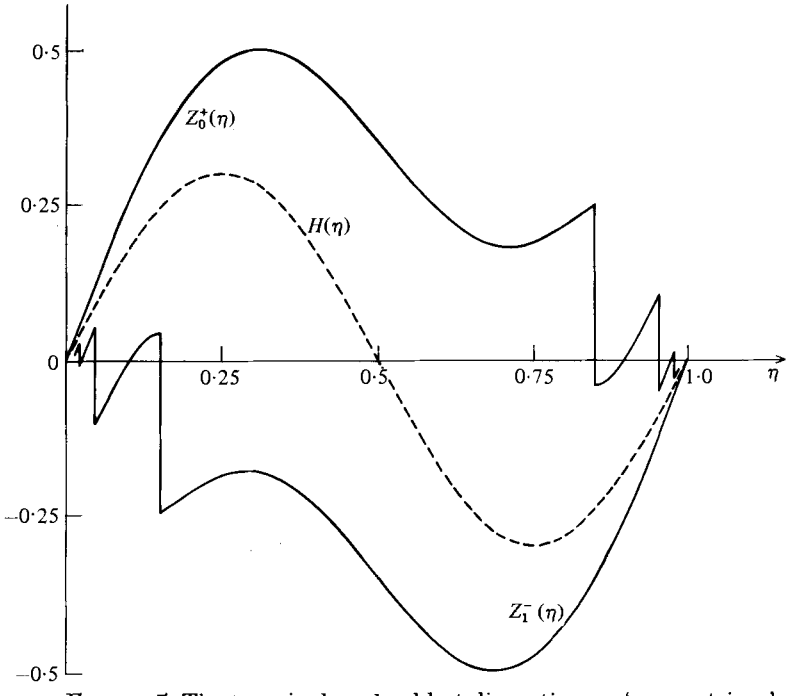

FIGURE 7. The two single-valued but discontinuous 'separatrices' on $[0, 1]$ $Z_0^+(\eta)$ and $Z_1^-(\eta)$ for $A = 0{\cdot}3$.

to η on $[0, 1]$, using equation (4.8) and the fact that H has zero mean value, again yields the equal-area rule (4.2) with Z replaced by F. Thus the discontinuity at x_s introduced by the mean condition is consistent with the weak shock conditions.

It remains to show that the composite function $F(\eta)$ defined by equation (4.6) is a solution of the functional equation (2.9). We define a second composite function

$$\hat{F}(\eta) = \begin{cases} Z_0^+(r(\eta)), & \eta = r + Z_0^+(r), \quad 0 \leqslant \eta < y, \\ Z_1^-(t(\eta)), & \eta = t + Z_1^-(t), \quad y \leqslant \eta < 1, \end{cases} \tag{4.9}$$

which is the distortion of $F(\eta)$ by the simple wave mapping $T1$. Then

$$\int_0^1 \hat{F}(\eta)\, d\eta = \int_0^1 F(\eta)\, d\eta = \Delta, \tag{4.10}$$

as required by equations (2.9), *only if* $y = x_s$. Hence the position and strength of the shock at $y = x_s$ are preserved under the full mapping (2.9), since H is continuous. Thus the composite function $F(\eta)$ defined by equation (4.6) is a discontinuous invariant curve. Note that the direction of the jump form Z_0^+ to Z_1^- results from the evolutionary nature of equations (2.9). A composite function with a jump from Z_0^- to Z_1^+ does not satisfy equations (2.9).

The function $\hat{F}(\eta)$ represents the distorted signal returning to the piston after reflexion from $x = 0$, but before it has been reinforced by the piston motion. Both $F(\eta)$ and $\hat{F}(\eta)$ are illustrated in figure 8 for the finite-rate case $A = 0{\cdot}50$.

Even in the small-rate range, with only a single shock at x_s, the distortion is

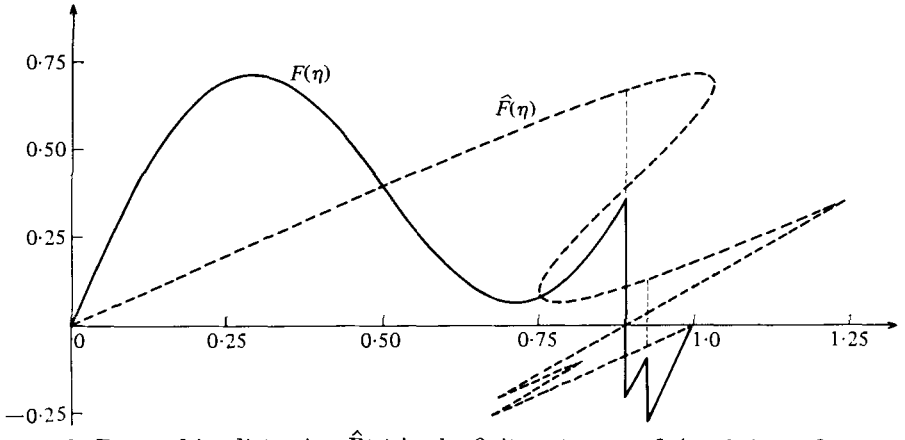

FIGURE 8. $F(\eta)$ and its distortion $\hat{F}(\eta)$ in the finite-rate case of $A = 0{\cdot}5$ at a frequency when F contains two shocks per period. $\hat{F}$ has shocks at the same locations with the same strengths as F.

appreciable. There is considerable distortion for $A = 0{\cdot}5$. During each cycle the two shocks which leave the piston coalesce before they return as the second shock, while a new shock is formed from the maximum values of $F(\eta)$. This always occurs in the finite-rate range at frequencies for which $F(\eta)$ contains more than one shock. It is important to note that the shock strengths and their locations, relative to the zeros of F, change as the signal traverses the tube. Only when the signal returns to the piston after a full cycle do the shock strengths and positions return to their original values. For example, if $F(\eta)$ contains two shocks on leaving the piston, there will in general be other locations in the tube where the corresponding $f(\beta)$ contains either one or three shocks.

5. Physical solutions

In this section we compare the finite-rate and small-rate invariants, F and F_d, in the linear resonance region and calculate the corresponding pressure variations on the piston. Only the functional equation (2.9) includes the effect of the continuous distortion of the signal as it moves in the tube. This results in discontinuous solutions in the linear resonance region which may contain any number of shocks, depending on the applied amplitude and frequency. The pressure variation calculated from F_d always contains only one shock per period.

We first contrast various properties of $Z_0^+(\eta)$ and $z^+(\eta)$, from which F and F_d are constructed. The separatrix $z^+(\eta)$ is symmetrical about $\eta = \frac{1}{2}$ for all A. Its maximum occurs at $\eta_m = \frac{1}{2}$ and is given by $z_m^+ = (2A\pi^{-1})^{\frac{1}{2}}$. The finite-rate separatrix $Z_0^+(\eta)$ is not symmetric and its maximum, Z_M^+, occurs at η_M, where $\frac{1}{2} - Z_0^+(\frac{1}{2}) < \eta_M < \frac{1}{2}$. When $A \ll 1$, $Z_M^+ \simeq z_m^+$; while, for $A \gg 1$, $Z_M^+ \sim A + \frac{1}{4}$. A good indicator of the difference in shape of $Z_0^+(\eta)$ and $z^+(\eta)$ is the position of the maximum, η_M, which decreases rapidly from 0·5 at $A = 0$ to 0·3 at $A = 0{\cdot}4$. As A increases further, η_M approaches 0·25. The corresponding linear invariant

$$F_l(\eta) = \Delta - \frac{A}{2\sin(\pi\Delta)}\cos(2\pi\eta + \pi\Delta), \tag{5.1}$$

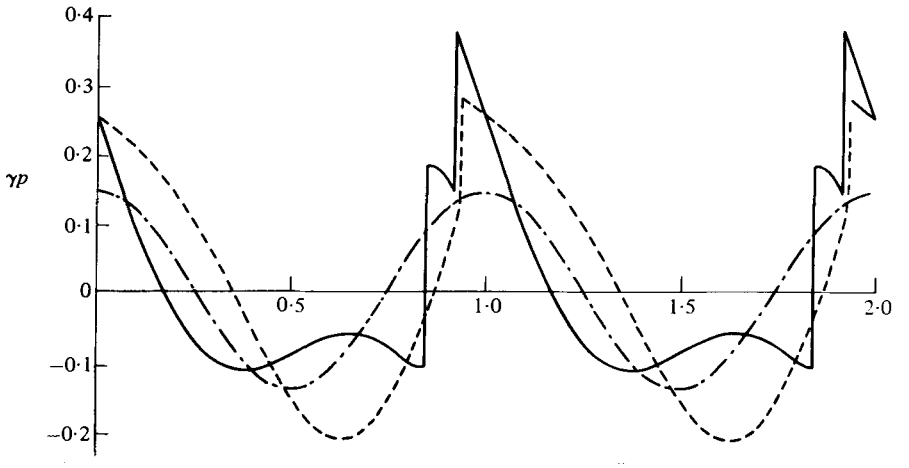

FIGURE 9. Pressure on the piston with $A = 0{\cdot}3$ for $\omega = 1{\cdot}128$ in the second mode, corresponding to $\epsilon = 0{\cdot}0156$. ——, present theory; ------, Chester's solution; –·–, linear theory.

is, of course, unbounded as $\Delta \to 0$. The linear maximum,

$$z_l(\Delta) = \Delta + A(2\sin(\pi\Delta))^{-1},$$

depends on both A and Δ. The maximum occurs at $\eta_l(\Delta) = \frac{1}{2}(1-\Delta)$.

The discrepancies between finite-rate, small-rate and linear theories are further illustrated by considering the variation in pressure on the piston. In calculating the invariants, using (2.9), (2.16) or (5.1), only A and Δ are specified, the solutions then being valid for any mode at the appropriate ϵ. When calculating the pressure the mode must also be specified, since the pressure on the piston is, by (2.5)–(2.8),

$$P(\eta) = (\omega M)^{-1}[\Delta + \tfrac{1}{2}A\sin(2\pi\eta) - F(\eta)]. \tag{5.2}$$

The small-rate pressure, $P_d(\eta)$, is also given by (5.2) with F replaced by F_d while the linear equivalent is

$$P_l(\eta) = (2\omega M)^{-1} A\cot(\pi\Delta)\cos(2\pi\eta). \tag{5.3}$$

For $|\Delta| < \Delta_e(A)$, $P_d(\eta)$ contains a single discontinuity in each period, while the number of discontinuities in $P(\eta)$ increases as $\Delta \to \Delta_l(A)$ for A large enough. However their strengths tend to zero as $\Delta \to \Delta_l$, and any form of damping could erase the smaller ones. P, P_d and P_l are compared in figure 9 for a typical amplitude of physical interest, $\epsilon = 0{\cdot}0156$, with the frequency $\omega = 1{\cdot}128$ ($\Delta = 0{\cdot}256$) in the second mode. These values give $A = 0{\cdot}3$, in the finite-rate range, $P_d(\eta)$ contains a single shock of strength $0{\cdot}126$ at $\eta = 0{\cdot}93$, while $P(\eta)$ contains two shocks of strengths $0{\cdot}218$ at $\eta_1 = 0{\cdot}82$ and $0{\cdot}176$ at $\eta_2 = 0{\cdot}92$. The small-rate theory concludes that a single shock of constant strength $0{\cdot}126$ travels in the tube. Since the finite-rate theory includes the intrinsic nonlinear distortion it predicts that the shock at η_1 will coalesce with that at η_2 as the signal traverses the tube. At the same time, a new shock, formed by the distortion of that part of the signal with slope $F' = -1$ (near $\eta = 0{\cdot}4$), evolves to take up its position at η_1 after one cycle.

Typical variations of pressure on the piston for several frequencies in the range $0{\cdot}872 \leqslant \omega \leqslant 1{\cdot}143$ of the second mode are illustrated in figure 10 when $\epsilon = 0{\cdot}024$. For this amplitude and range of frequencies, A varies from $0{\cdot}275$ to $0{\cdot}473$. The corresponding response curve, indicating maximum and minimum pressures and shock strengths at the piston, is given in figure 11.

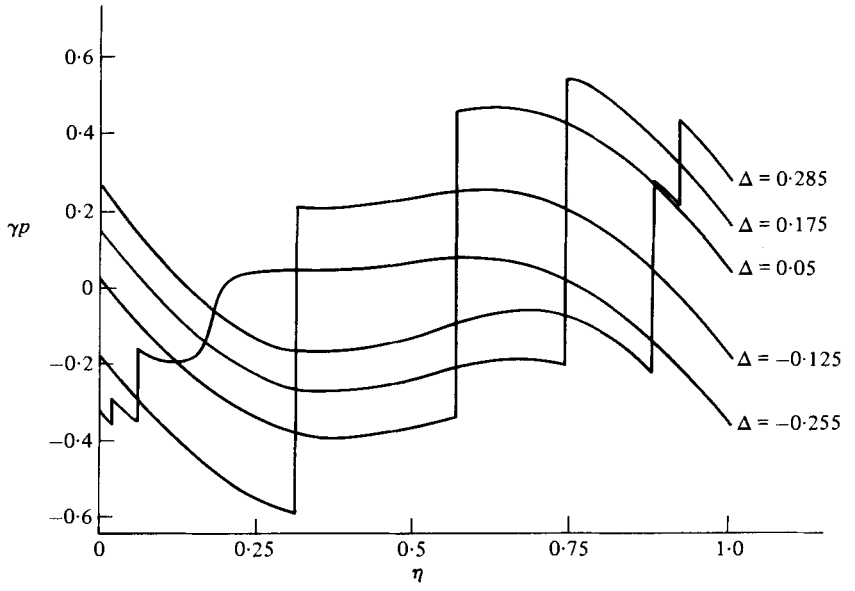

FIGURE 10. Pressure on the piston for several frequencies in the range $0{\cdot}872 \leqslant \omega \leqslant 1{\cdot}143$ when $\epsilon = 0{\cdot}024$. They correspond to $\Delta = 0{\cdot}255$, $-0{\cdot}125$, $0{\cdot}05$, $0{\cdot}175$ and $0{\cdot}285$ with $0{\cdot}275 \leqslant A \leqslant 0{\cdot}473$.

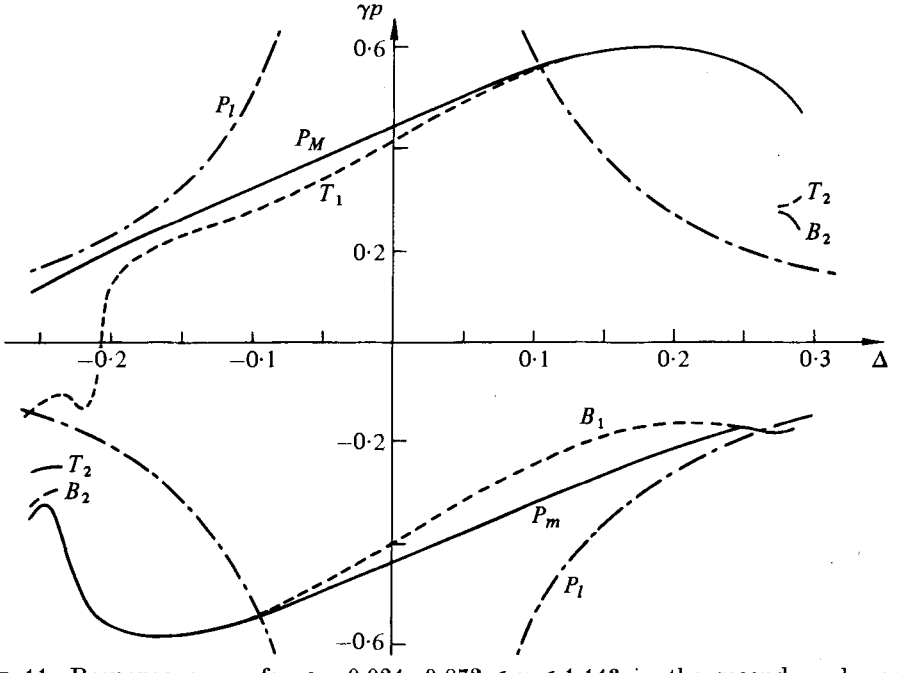

FIGURE 11. Response curve for $\epsilon = 0{\cdot}024$, $0{\cdot}872 \leqslant \omega \leqslant 1{\cdot}143$ in the second mode, so that $\Delta = 2(\omega - 1)$. Curves indicate maximum pressure P_M, minimum pressure P_m, pressure at top and bottom of shocks, $T_{1,2}$ and $B_{1,2}$, and linear maximum and minimum pressure P_l.

Continuous solutions of the functional equation (2.9) are constructed in Mortell & Seymour (1979) for values of A and Δ inside the transition curve of figure 1, while here we have found the discontinuous solutions in the linear resonance region. These discontinuous solutions satisfy the weak shock conditions because of the evolutionary nature of equation (2.9). However, the critical point technique introduced in § 3 will yield a solution only in that region of the A–Δ plane for which there is an amplitude of the propagating signal which completes a cycle in the tube in an integer multiple of the period. Outside the linear resonance region, for example when Δ is in the neighbourhood of 0·5, the formulation of the problem must be modified before an extension of the concept of a critical point yields the solution. This analysis applied to the problem of nonlinear resonance is the subject of our next paper.

The authors thank Mr Wolfgang Richter for his invaluable programming assistance and one of the referees for his constructive comments. This work was supported in part by the Natural Sciences and Engineering Research Council of Canada under Grant A9117, and was completed while one of the authors (B.R.S.) held an S.R.C. Senior Visiting Fellowship at the University of Oxford.

REFERENCES

BETCHOV, R. 1958 Nonlinear oscillations of a column of gas. *Phys. Fluids* **1**, 205–212.

BROCHER, E. 1977 Oscillatory flows in ducts: a report on Euromech 73. *J. Fluid Mech.* **79**, 113–126.

CHESTER, W. 1964 Resonant oscillations in closed tubes. *J. Fluid Mech.* **18**, 44–64.

GALIEV, S. U., ILGAMOV, M. A. & SADYKOV, A. V. 1970 Periodic shock waves in a gas. *Isv. Akad. Nauk S.S.S.R. Mech. Zhid. i Gaza* **2**, 57–66.

GORKOV, L. P. 1963 Nonlinear acoustic oscillations of a gas column within an enclosed duct. *Ingenernij J.* **3**, 246–250.

GULYAYEV, A. I. & KUSNETSOV, W. T. 1963 Gas oscillations with finite amplitude in a closed tube. *Ingenernij J.* **3**, 216–245.

KUCZMA, M. 1968 *Functional Equations in a Single Variable.* Warsaw: PWN.

LETTAU, E. 1939 Messungen an Gasschwingungen grosser Amplitude in Rohrleitungen. *Deutsche Kraftfahrforschung* **39**, 1–17.

MORTELL, M. P. 1971 Resonant thermal-acoustic oscillations. *Int. J. Engng Sci.* **9**, 175–192.

MORTELL, M. P. & SEYMOUR, B. R. 1976 Exact solutions of a functional equation arising in nonlinear wave propagation. *SIAM J. Appl. Math.* **30**, 587–596.

MORTELL, M. P. & SEYMOUR, B. R. 1979 Nonlinear forced oscillations in a closed tube: continuous solutions of a functional equation. *Proc. Roy. Soc.* A **367**, 253–270.

MORTELL, M. P. & SEYMOUR, B. R. 1980 A finite rate theory of quadratic resonance. In preparation.

SAENGER, R. A. & HUDSON, G. E. 1960 Periodic shock waves in resonating gas columns. *J. Acoust. Soc. Am.* **32**, 961–970.

SEYMOUR, B. R. & MORTELL, M. P. 1973 Resonant acoustic oscillations with damping: small rate theory. *J. Fluid Mech.* **58**, 353–373.

STURTEVANT, B. 1974 Nonlinear gas oscillations in pipes. Part 2. Experiment. *J. Fluid Mec.* **63**, 97–120.

WHITHAM, G. 1974 *Linear and Nonlinear Waves.* Wiley-Interscience.

ZAPIROV, R. G. & ILGAMOV, M. A. 1976 Nonlinear gas oscillations in a pipe. *J. Sound Vib.* **46**, 245–257.